Evolutionary genomics predicts probiotic persistence in corals

Mei Xie[1]†, Nan Xiang[1]†, Tianhua Liao[1]†, Chun Ting Cheung[1], Zhihao Xian[1], Pan Li[1], Chi Hin Lee[1], Wai Yin Tse[1], Kwong Kit Tsang[1], Congjuan Xu[1], Kaitlyn E. Ho[1], Qian He[1], Melanie Dörr[2], Hannah Manns[2], Xiaojun Wang[1], Danli Luo[1], Róisín Hayden[3,4], Emily Chei[3,4], Zhongyue Wan[3,4], Philip Thompson[3,4], Joseph Brennan[3,4], Raquel S. Peixoto[5], Guoxin Cui[5], Shelby E. McIlroy[1,3,4], Apple Pui Yi Chui[1], Christian R. Voolstra[2], Haiwei Luo[1,6,7,8]*

[1]Simon F. S. Li Marine Science Laboratory, School of Life Sciences, The Chinese University of Hong Kong; Shatin, Hong Kong SAR.

[2]Department of Biology, University of Konstanz; Konstanz, Germany.

[3]The Swire Institute of Marine Science, The University of Hong Kong; Cape D'Aguilar Road, Shek O, Hong Kong SAR.

[4]School of Biological Sciences, The University of Hong Kong; Pok Fu Lam, Hong Kong SAR.

[5]Division of Biological and Environmental Science and Engineering (BESE), Red Sea Research Center, King Abdullah University of Science and Technology (KAUST); Thuwal, Saudi Arabia.

[6]State Key Laboratory of Agrobiotechnology, The Chinese University of Hong Kong; Shatin, Hong Kong SAR.

[7]Department of Earth and Environmental Sciences, The Chinese University of Hong Kong; Shatin, Hong Kong SAR.

[8]Institute of Environment, Energy and Sustainability, The Chinese University of Hong Kong; Shatin, Hong Kong SAR.

†These authors contributed equally to this work.

***Corresponding author:**

E-mail: haiweiluo@cuhk.edu.hk

Abstract

A universal bottleneck limiting probiotic efficacy in medicine, aquaculture, agriculture, and wildlife conservation is uncertain long-term colonization, necessitating repeated administration. We present an evolution-guided framework for probiotic identification based on genomic hallmarks of emerging host dependency, including widespread pseudogenization and insertion sequence proliferation driving genomic restructuring. Applied to coral reefs, we screened over 1,200 coral-associated bacterial isolates and identified *Ruegeria* MC10 as exhibiting these signatures. Its presence was associated with increased thermal tolerance of a model cnidarian. Following nursery application, MC10 persisted in reef corals for an 8-month monitoring period through a natural bleaching event, improving color retention and retaining algal photosynthesis performance. This work establishes a predictive, scalable pipeline for selecting persistent probiotics, directly addressing a central constraint on microbiome-based interventions across host systems.

Main Text

Probiotics, defined as live microorganisms administered to confer health benefits, hold transformative potential across diverse fields from human medicine to wildlife conservation (*1-4*). A pervasive challenge limits their long-term efficacy and large-scale application: most administered microbes fail to establish stable, enduring colonization within host-associated microbiomes (*1, 2, 5-8*). This bottleneck necessitates repeated, costly, and often impractical reapplication, undermining the promise of probiotics as sustainable interventions.

Evolutionary genomics can provide a predictive solution to this colonization challenge. As bacteria transition from a free-living to a host-dependent lifestyle, their genomes undergo characteristic restructuring. Key hallmarks include the proliferation of insertion sequences (IS), mobile genetic elements that act as engines of genomic plasticity, coupled with the pseudogenization of core metabolic pathways (*9, 10*). These signatures reflect an evolutionary trajectory toward host dependency, where metabolic reliance can reinforce a persistent symbiotic association. We therefore hypothesize that probiotic candidates selected *a priori* for these genomic features possess an intrinsic predisposition for long-term host residency.

Coral reefs present a critically threatened and functionally relevant system in which to test this predictive framework. These ecosystems sustain immense biodiversity and human livelihoods, but these ecosystems are collapsing under climate change (*11-13*). Since the 1950s, an estimated half of global coral cover has been lost (*14*). Even under the 1.5 °C Paris Agreement target, 70-90% of coral reefs are projected to be lost by 2050 (*15*). The breakdown of the coral-algal symbiosis during thermal stress triggers coral bleaching and subsequent mortality (*16*). The accelerating frequency of mass bleaching events, including the catastrophic global events of 2014-2017 (*17*) and 2023-2025 (*18*), has left reefs with insufficient recovery intervals,

necessitating active interventions to enhance resilience.

Here, we apply an evolutionary selection strategy to *Ruegeria*, a common bacterial genus member of coral holobionts (*19, 20*). From a collection of over 1,200 coral-associated bacterial isolates, we identified a *Ruegeria* population, MC10, exhibiting genomic signatures of early-stage host dependency. Exposure to MC10 was associated with increased thermal tolerance in a model cnidarian. Following nursery inoculation with no subsequent reapplication, we deployed MC10- and placebo-treated coral in an eight-month field trial encompassing a natural bleaching event. We demonstrate that this candidate achieved sustained colonization *in hospite* that increased host thermal resilience. This work establishes a generalizable, predictive pipeline for selecting enduring probiotics, offering a solution to a universal probiotic limitation and providing a timely, scalable tool for ecosystem resilience.

Results

Ruegeria population MC10 as a putative next-generation coral probiotic

To identify candidate probiotics exhibiting genomic hallmarks of host dependency, we cultured 419 *Ruegeria* isolates from five coral species (*Acropora* cf. *samoensis*, *Acropora solitaryensis*, *Favites pentagona*, *Platygyra acuta*, and *Oulastrea crispata*) collected across nine sites spanning environmental gradients in Hong Kong (**Fig. S1**). Bacterial isolates were primarily obtained from coral mucus and skeleton (**Fig. 1A**), sampling from potentially transient surface associates to more persistent tissue- and skeleton-associated taxa.

Using PopCOGenT, a method that delineates populations (main clusters, MCs) based on recombination barriers without phylogenetic tree input (*21*), we resolved 116 genetically cohesive *Ruegeria* populations, 29 of which contained at least 3 isolates (**Fig. 1A**).

Phylogenomic analysis confirmed monophyly for most, validating PopCOGenT's accuracy for tracking probiotic diversity at an ecologically meaningful unit. Among these, population MC10 emerged as a prime candidate. To accurately identify genomic hallmarks of evolutionary recent endosymbionts, specifically insertion sequence (IS) expansion (**Fig. 1B**) and pseudogene proliferation (**Fig. 1C**), we analyzed closed genome assemblies (**Fig. S2**). These analyses revealed frameshift and nonsense mutations disrupting genes across multiple essential metabolic pathways. Disruptions in the tricarboxylic acid (TCA) cycle were prominent, affecting genes including aconitate hydratase (*ACO*), isocitrate dehydrogenase (*IDH1*), succinyl-CoA synthetase (*sucC*), malate dehydrogenase (*mdh*), and succinate dehydrogenase (*sdhA*) (**Fig. S3**). The location of these mutations suggests a gradient of functional impact: 5'-terminal disruptions are expected to severely impair protein function, whereas mutations nearer the 3' terminus may allow for partially functional gene products. This spectrum of mutational effects likely underpins the retained, albeit reduced, metabolic capacity enabling MC10's culturability (**Fig. S3** & **Fig. S4**). Pseudogenization was not restricted to the TCA cycle but was widespread across glycolysis, the pentose phosphate pathway, gluconeogenesis, amino acid biosynthesis, and vitamin and cofactor synthesis pathways (**Fig. S5**). These pseudogenized loci typically lacked functional paralogs, suggesting a potential heightened metabolic reliance on the coral host. These signatures were almost exclusively found in MC10 and were absent in other *Ruegeria* populations.

Within MC10, we observed functional heterogeneity in these hallmark signatures. Some strains (e.g., MC10-B4) exhibited extensive pseudogenization across the pathways described, whereas others (e.g., MC10-AJ1) retained largely complete pathways (**Fig. S5**). This within-population variation presents a potential source of difference in strain-level efficacy. MC10 collectively exemplifies the defining genomic features of a next-generation probiotic candidate: pronounced

IS-driven genomic restructuring coupled with expanded pseudogenization (**Fig. 1C**), hallmarks of a lineage transitioning toward host dependency. Phylogenetically, MC10's closest relative is MC46 (**Fig. 1A**), which shares 99.45% 16S rRNA gene identity but diverges genomically (average nucleotide identity: 86.88 ± 0.04%; **Fig. S6**) and lacks IS expansion or widespread pseudogenization (**Fig. 1B & 1C**). This contrast underscores MC10's distinct genomic trajectory toward host association.

Reduced free-living growth distinguishes Ruegeria MC10 from related populations

The genomic hallmarks of early-stage host-dependency prompted us to investigate whether this evolutionary trajectory is associated with a physiological cost to free-living growth. We performed a phylogenetically-informed comparison of maximum growth rates (μ_{max}) across a diverse panel of 24 *Ruegeria* isolates (**Fig. 1A**). This panel included three strains from population MC10, representing its spectrum of pseudogenization from the extensively pseudogenized MC10-B4 to isolates (e.g., MC10-AJ1) with minimal pseudogenization in essential pathways, all sampled from distinct reef sites; two strains from its sister population MC46; and 18 phylogenetically diverse strains from 18 other *Ruegeria* MCs spanning various hosts, compartments, and sites, plus the free-living model *R. pomeroyi* DSS-3 (*22*).

Consistent with predicted metabolic constraints arising from pseudogenization, members of population MC10 exhibited significantly lower maximum growth rates compared to all other *Ruegeria* populations under standardized laboratory conditions (Phylogenetic ANOVA, Brownian motion model, $P = 0.009$; **Fig. 1D and S7**; **Table S1**). This reduction was particularly evident when comparing MC10 to its closest relative, MC46, which lacks IS expansion and pseudogene proliferation (**Fig. 1B & 1C**). MC46 strains displayed substantially higher growth

rates, underscoring that the attenuated growth is a specific phenotypic correlate of MC10's unique genomic trajectory toward host association, rather than a shared trait of closely related lineages.

Despite this constraint on growth rate, MC10 remains fully culturable and achieves a robust cell yield. The representative strain MC10-B4 (μ_{max} = 0.12 h^{-1}) reached a stationary-phase density of 9.92 ± 0.14 Log_{10} CFU/mL, which was significantly higher than the yields of the sympatric control strain MC15-BG7 (9.44 ± 0.03 Log_{10} CFU/mL) and the model *R. pomeroyi* DSS-3 (9.25 ± 0.10 Log_{10} CFU/mL).

Ruegeria MC10 is present across diverse coral species

To assess the ecological distribution and host associations of *Ruegeria* MC10, we performed targeted amplicon sequencing of two population-resolving marker genes, *parC* (encoding a topoisomerase IV subunit) and *ATP5B* (encoding an ATP synthase subunit). These markers were selected from over 700 conserved single-copy *Ruegeria* gene families and validated for their ability to resolve PopCOGenT-defined populations into monophyletic groups (**Fig. S8**). Custom primers achieved high recovery rates (64.8% for *parC*; 74.3% for *ATP5B*; **Table S2**), enabling sensitive detection across samples.

Although pure cultures of MC10 were originally sourced from *Oulastrea crispata* (**Fig. 1A**), culture-independent amplicon data revealed its presence in all five coral species (*Oulastrea crispata*, *Acropora solitaryensis*, *Plesiastrea versipora*, *Porites* sp., and *Platygyra acuta*) sampled from multiple Hong Kong reef sites, as well as in seawater and sediment samples (**Fig. 2**). Detection varied among colonies of the same species. Where present, MC10 typically constituted <2% of the local *Ruegeria* communities. Estimates of its relative abundance based

on *parC* and *ATP5B* markers showed no linear correlation at low proportions (<0.5%; **Fig. S9**), reflecting methodological challenges in quantifying low-abundance populations. We also attempted to quantify absolute abundance via qPCR but did not obtain reliable signals (**Fig. S10**).

Ruegeria MC10 exposure is associated with increased thermal tolerance of a model cnidarian

To probe MC10's probiotic potential, we used the standardized Coral Bleaching Automated Stress System (CBASS) to conduct short-term heat stress assays (*23*, *24*). We exposed individuals of the sea anemone Aiptasia (sensu *Exaiptasia diaphana*, a model for coral-algal symbiosis) (*25*) to the strain MC10-B4 at a pre-screened concentration of 10^6 CFU/ml for 24 hours (**Fig. S11**) prior to thermal stress testing (**Fig. S12**). The CBASS protocol involved a 3-hour temperature ramp from 30 °C to target levels (34 °C, 36 °C, or 39 °C) under light, a 3-hour hold, a 1-hour ramp-down to 30 °C in darkness, and an 11-hour overnight reprieve (*24*). Dark-acclimated photosynthetic efficiency (F_v/F_m) was measured at T7 (7th hour, post-stress) to assess thermal tolerance and at T18 (18th hour, post-overnight recovery) to evaluate resilience capacity (*24*). Thermal tolerance was quantified using the Effective Dose 50 (ED50), defined as the temperature causing a 50% decline in F_v/F_m relative to unstressed controls (*26*).

MC10-inoculated Aiptasia exhibited a significant increase in thermal tolerance compared to placebo (filtered seawater) controls, with a 1 °C higher ED50 at T7 (P = 0.001, Student's t-test) and a 0.6 °C increase at T18 (P = 0.013) (**Fig. 3A & 3B, Table S3**). While transient nutritional benefits from the bacterial inoculum cannot be entirely ruled out in such an acute assay, this result provided preliminary evidence of a beneficial physiological outcome under acute stress and confirmed the non-pathogenic nature of MC10-B4 in this model system.

Sustained association and thermal tolerance in reef corals following Ruegeria MC10 application

Prior to field deployment, we assessed the colonization capacity predicted by MC10's evolutionary genomics profile. In a controlled *ex situ* assay, nubbins derived from multiple *Acropora pruinosa* colonies (with fragments from each colony distributed across treatments) received twice-weekly inoculations over four weeks with strain MC10-B4, the sympatric control strain MC15-BG7 (isolated from the same coral colony and compartment), or an autoclaved filtered seawater (AFSW) placebo. Amplicon sequencing revealed that MC10-B4 achieved a median relative abundance of 18.331% within the coral *Ruegeria* community (0.003% of total bacteria), significantly higher than the placebo (2.410% of *Ruegeria*, <0.001% total bacteria; P = 0.002 and P = 0.007, respectively; one-way ANOVA; **Fig. 3C**, **Table S4**). In contrast, corals inoculated with MC15-BG7 showed no significant increase in MC15 abundance (median 3.242% of *Ruegeria*, <0.001% total bacteria) over the placebo control (0.251% of *Ruegeria*, <0.001% total bacteria; P = 0.136 and 0.281; **Fig. 3D**, **Table S4**).

Following this *ex situ* validation, MC10-B4-inoculated and placebo-treated *A. pruinosa* fragments were outplanted to adjacent reef sites (40 m apart) in January 2024 (**Fig. S13**). Corals were monitored over eight months at defined timepoints: after nursery inoculation but before outplanting (**t0**), and at 1, 3, 6, 7, and 8 months post-outplanting (**t1**, **t3**, **t6**, **t7**, **t8**). A natural, region-wide bleaching event occurred between July and September 2024, during which degree heating weeks (DHW) reached 8.8-18 ºC-weeks (**Fig. S14**), exceeding established NOAA bleaching thresholds.

MC10-B4-inoculated corals exhibited enhanced thermal tolerance specifically during the natural bleaching event. At the peak of thermal stress (**t6** and **t7**), probiotic-treated corals showed

significantly reduced bleaching severity compared to placebo controls (CoralWatch Coral Health Chart coloration scores at **t6**: 3.3 ± 0.5 vs. 2.5 ± 0.4, $P < 0.001$; **t7**: 3.2 ± 0.4 vs. 2.4 ± 0.4, $P < 0.001$; two-way ANOVA, Tukey's HSD; **Fig. 3E, Table S5**). The operational efficiency of PSII under ambient light conditions (F_v'/F_m') was also significantly higher in the probiotic group during this period (**t6**: $P < 0.001$; **t7**: $P < 0.001$; two-way ANOVA, Tukey's HSD; **Fig. 3F, Table S6**). A significant treatment-by-time interaction ($P < 0.001$, two-way ANOVA, interaction effect) indicated that the probiotic's effect was contingent on the presence of thermal stress. Following the thermal stress peak but with DHW levels still elevated above stress-relief thresholds at **t8**, both groups exhibited partial recoloration.

To investigate the mechanism underlying the observed thermal resilience, we conducted a control experiment to exclude potential effects from nutritional supplementation, transient priming by live cells, or postbiotic contributions from bacterial components and metabolites. *Acropora pruinosa* nubbins were exposed for 28 days to live, autoclaved, or pasteurized cells of MC10-B4 and MC15-BG7, using the same twice-weekly inoculation scheme applied in the nursery. An AFSW placebo control was included, yielding seven experimental groups in total. A holistic physiological assessment showed that live inoculation with either bacterial strain did not alter the coral's baseline state across key metrics, including photosynthetic efficiency (F_v/F_m), coloration, host protein content (per surface area), total lipid energy content (per dry weight), chlorophyll a concentration (per surface area), symbiont density (per surface area), and host fluorescent protein content (Relative Fluorescence Units per host protein weight), compared to the placebo control (two-way ANOVA, Tukey's HSD, $P > 0.05$; **Fig. S15, Table S7**). Isolated changes were observed in fragments exposed to pasteurized MC10-B4 cells, which exhibited a reduction in F_v/F_m and an increase in host fluorescent protein content compared to placebo

controls (*P* = 0.004 and 0.001, respectively). In contrast, fragments exposed to pasteurized MC15-BG7 showed a significant increase in total lipid energy content (*P* = 0.003). These effects were not observed with pasteurized counterparts of the other strain or with autoclave-killed cells of either strain.

To visually confirm the persistent presence of MC10 within host tissues, we used fluorescence *in situ* hybridization (FISH) with a population-specific probe. Because conventional 16S rRNA probes lack the resolution to distinguish MC10 from other *Ruegeria* populations, we developed a 215 bp probe targeting the single-copy *parC* gene. Probe specificity was validated using pure cultures of MC10-B4 (**Fig. S16**). In coral samples collected immediately after nursery inoculation (**t0**) and at six (**t6**) and eight (**t8**) months post-outplanting, the probe revealed MC10 cells localized within the coral gastrodermis (**Fig. 3G**). Specificity in holobiont samples was confirmed using a nonsense probe control (**Fig. 3G**). MC10 was not necessarily co-localized with Symbiodiniaceae. The low natural abundance of MC10 within *Ruegeria* communities (median 0.23%) and of *Ruegeria* within total coral microbiomes (median 0.02%) precluded precise quantification via amplicon sequencing, falling below typical detection threshold (0.5%) for reliable amplicon sequence variant (ASV) resolution (*27*).

Bacterial community dynamics in outplanted corals were assessed via *parC* and 16S rRNA gene amplicon sequencing at multiple timepoints (**t0, t1, t3, t6**, and **t8**; **t7** samples unavailable). Analysis of β-diversity revealed that bacterial communities in MC10-B4-inoculated corals became progressively more similar to those in placebo corals over the monitoring period (**Fig. 4A**; ANOSIM). During the peak bleaching phase (**t6**), genus-level analysis identified a significant enrichment of several Bacteroidetes genera (*Cryomorpha*, *Spirosoma*, *Sunxiuqinia*, *Gelatiniphilus*, *Aureispira*, and *Flavobacterium*) and a depletion of multiple Roseobacteraceae

genera (*Sulfitobacter*, *Roseovarius*, *Pseudoruegeria*, *Donghicola*, *Aliiroseovarius*, and *Phaeobacter*) in MC10-B4-inoculated corals compared to the placebo group (FDR-corrected $P < 0.05$; ANCOM-BC; **Fig. 4B**). Most of these taxa showed no differential abundance during pre-bleaching (**t3**) or post-bleaching (**t8**) phases (**Fig. S17**), indicating that MC10 inoculation was associated with a specific restructuring of the coral microbiome during thermal stress.

Discussion

The accelerating loss of biodiversity under climate change demands innovative strategies to enhance ecosystem resilience. Probiotics have shown promise, yet their long-term efficacy is often limited by transient colonization, a fundamental limitation on scalable *in situ* application (*1, 2, 5-8*). Here, we propose and validate a framework to overcome this challenge: the selection of probiotic candidates based on evolutionary genomic signatures indicative of a transition towards host dependency, which predicts stable host association. We demonstrate this framework in the context of coral reefs. Focusing on the coral-associated bacterial genus *Ruegeria* (*19, 20*), we identified population MC10, which exhibits hallmarks of early-stage host dependency. A nursery inoculation enabled MC10 to be retained in coral tissues throughout an 8-month field trial, where its persistent colonization conferred increased host thermal resilience during a natural bleaching event. This work establishes a predictive probiotic selection pipeline that combines evolutionary trajectory with functional validation.

Evolutionary genomic signatures as predictors of probiotic persistence

Common approaches to selecting marine probiotics have primarily relied on screening for functional traits such as pathogen inhibition, ROS degradation, or nutrient provisioning (*28, 29*),

with the hope that selected strains will persist in the host. A key limitation for scalable application, however, is the uncertainty regarding their long-term residency within host tissues (*30*). Our framework inverts this process: we first select for evolutionary signatures predictive of stable colonization, and then empirically test whether the persistent strain provides a host benefit.

This strategy is grounded in the hypothesis that specific genomic signatures predict a bacterial lineage's propensity for stable host association. In MC10, we observed hallmarks of genomic restructuring and decay, including IS expansion and pseudogene proliferation. IS proliferation serves as an engine of genomic plasticity, facilitating deletions and rearrangements that accelerate host adaptation (*31, 32*). This state enables the fixation of conditionally deleterious mutations, such as those disrupting core metabolism in MC10. Such genomic restructuring incurs a defined phenotypic cost: MC10 exhibited a significantly reduced maximum growth rate under free-living conditions compared to related *Ruegeria* populations. This attenuated independent proliferation capacity phenotypically validates the genomic trajectory toward host dependency. The resulting metabolic reliance reinforces symbiosis, transforming a physiological cost in one environment into a stabilizing mechanism in another.

The genomic signatures observed in *Ruegeria* MC10 mirror those in terrestrial model symbionts such as *Sodalis glossinidius*, where they signify a transitional state toward host dependency (*9, 10*). Proactively applying these evolutionary principles to select probiotics represents a distinct strategy for conservation. Our study tests the key functional implication: that this genomic trajectory facilitates stable, long-term association. Supporting this, a companion trait study (*33*) reveals that MC10's genomic architecture is coupled with a functional profile conducive to host residency, including robust biofilm formation and host-induced "motility-to-sessility" proteomic reprogramming, responses not observed in sympatric *Ruegeria* isolates like

MC15-BG7. The sustained colonization and enhanced thermal resilience demonstrated by *Ruegeria* MC10 confirm the feasibility of this evolution-guided approach.

Validating the framework: From laboratory predictions to field trial design

A primary objective of this work was to introduce and provide a first field validation for a two-part selection framework. This framework first employs evolutionary genomics to identify probiotic candidates with a high *a priori* potential for sustained host colonization, and then requires empirical testing to confirm that such persistent candidates deliver a measurable host benefit. The proof-of-concept lies in demonstrating that a candidate (MC10-B4) chosen specifically for its genomic signatures can achieve sustained retention and confer beneficial host effects in a real-world setting. Consequently, the field trial was designed to include a placebo control. The objective was not to benchmark MC10 against alternative candidates, but to test whether an evolutionarily informed selection framework can prospectively identify a probiotic with a high probability of sustained colonization and functional benefit under field conditions. A successful outcome validates the framework as a strategy for de-risking probiotic selection.

We designed controlled laboratory experiments to rule out alternative explanations for a potential probiotic benefit. The nutritional contribution of the inoculum was negligible because the total dose delivered (~10^7 cells/mL per fragment twice a week over four weeks) was orders of magnitude lower than the ambient bacterial load in the rearing system (~3×10^{11} cells in a 200 L volume at ~1.5×10^6 cells/mL). MC10-B4 established at significantly higher levels in *Acropora pruinosa* than the sympatric control strain MC15-BG7, confirming that this colonization capacity was aligned with MC10's genomic predisposition for persistent residency, rather than being a general trait of coral-associated *Ruegeria*. Live inoculation with either MC10-

B4 or MC15-BG7 did not alter baseline coral physiology across physiological metrics, including photosynthetic efficiency, coloration, host protein content, total lipid energy content, chlorophyll a concentration, symbiont density, and host fluorescent protein content, compared to an AFSW placebo, which ruled out an inoculation-induced priming effect, independent of sustained colonization, as the cause of later field-observed benefits.

The field trial tested the core prediction that persistent colonization by MC10-B4 would enhance host thermal resilience. Treatments were deployed at separate but proximate sites (~40 m apart) within the same habitat, minimizing the risk of cross-contamination via passive dispersal while ensuring similar environmental conditions (depth 4 m; sand-rubble substrate; tide-driven flow, 0.2±0.3 m/s, (*34*)). At this scale, water depth, rather than along-reef distance, primarily structures environmental variability on coral reefs (*35*-*37*). Baseline monitoring confirmed that key abiotic parameters, including water temperature and dissolved inorganic nitrogen, were statistically indistinguishable between sites. The primary environmental driver during the observation period was an extreme, regional heat stress event (DHW 8.8-18 °C-weeks).

To exclude postbiotic effects, we compared coral responses to live, autoclaved, and pasteurized bacterial cells. This experiment revealed two distinct outcomes. Exposure to pasteurized MC10-B4 cells, which are expected to preserve some heat-labile metabolites, reduced photosynthetic efficiency. This effect contrasts with the relative preservation of photosynthetic efficiency observed in MC10-inoculated corals under field stress. This result indicates that a one-time release of heat-labile metabolites cannot explain the beneficial outcome observed in the field. The same treatment increased host fluorescent protein content, a response associated with antioxidant capacity. One interpretation is that specific MC10 metabolites could

initiate a beneficial stress-response priming in the holobiont. These responses were not observed with live MC10-B4, nor with pasteurized MC15-BG7 or autoclave-killed cells. Therefore, even if certain metabolites could theoretically prime the host, for such priming to provide protection during a bleaching event months later would require the continual presence of the metabolite source: a persistently resident bacterial population. Thus, any integrated ‘probiotic-postbiotic’ mechanism fundamentally depends on the sustained colonization that our evolutionary framework selects for.

Collectively, these experiments argued against mechanisms relying on nutrition, transient priming, or one-time postbiotic effects. The treatment-specific benefits observed during peak thermal stress, supported by mechanistic dissection, indicate that sustained colonization was the underlying cause. This validates the core prediction of our evolution-guided framework.

Facultative endosymbionts as host-generalist probiotics

Ruegeria MC10 can be described as a facultative endosymbiont, given its variable occurrence among conspecific coral colonies and its detection in free-living environments. Such facultative symbionts exhibit a distinctive duality: genomic erosion drives metabolic dependency whereas ecological flexibility is retained. This life history strategy may enable a broad host range.

MC10’s host versatility could arise from mechanisms that exploit conserved host interfaces rather than lineage-specific adaptations. For instance, strain MC10-B4’s pseudogenized TCA cycle necessitates scavenging host-derived metabolites like succinate or fumarate, pathways conserved across eukaryotes. This strategy aligns with “resource tracking”, a mechanism whereby symbionts exploit universal host resources to colonize diverse hosts (*38*). Colonization could also involve interactions with conserved eukaryotic cell interfaces, a concept reminiscent

of generalist probiotics like *Lactiplantibacillus plantarum*, which uses a conserved colonization island to inhabit hosts from *Drosophila* to humans (*39*). This aligns with "ecological fitting", where pre-existing traits enable colonization of novel hosts without coevolution, a key driver of host generalization in facultative symbioses (*38*).

MC10's persistence in the environment alongside corals could reflect relatively weak host selection pressures. When hosts impose minimal filtering, symbionts face reduced costs of adaptation to novel hosts, facilitating niche expansion (*38*). MC10's low relative abundance in coral microbiomes likely minimizes its burden on the host, potentially weakening selection for specialization. The scalability of this probiotic approach is enhanced by such generalism. Unlike obligate symbionts restricted to single hosts (*10*), facultative endosymbionts like MC10 may exploit conserved molecular gateways, enabling nursery-based priming of diverse coral species with a single probiotic preparation.

Microbiome dynamics and stability

A central goal of probiotic intervention aligns with microbial transfer therapy in human medical settings: introducing beneficial taxa to reset dysbiotic microbiomes and enhance resilience through targeted restructuring (*20, 40*). Using *Ruegeria* MC10 as a keystone inoculant, we observed microbiome modulation without long-term destabilization. While β-diversity differences between probiotic-inoculated and placebo-treated corals peaked post-inoculation, communities converged over the monitoring period, indicating environmental acclimatization.

During the peak of bleaching stress (**t6**), the presence of MC10-B4 was associated with a specific restructuring of the coral microbiome. Analysis revealed significant enrichment of Bacteroidetes taxa specializing in polysaccharide degradation (*Cryomorpha*, *Spirosoma*,

Sunxiuqinia, *Gelatiniphilus*, *Aureispira*, *Flavobacterium*) (*41*), ROS-tolerant genera (*Deinococcus*, *Desertibacter*, *Spirosoma*) (*42*), the *Vibrio*-predatory specialist (*Aureispira*) (*43*), and known probiotic taxa (*Veillonella*, *Limosilactobacillus*) (*44*, *45*). Concurrently, multiple Roseobacteraceae genera were depleted (*Sulfitobacter*, *Roseovarius*, *Pseudoruegeria*, *Donghicola*, *Aliiroseovarius*, *Phaeobacter*). This depletion may indicate competitive restructuring within this family or may reflect their close association with Symbiodinaceae (*46*), which are themselves stressed and declining during bleaching. These shifts were largely absent before (**t3**) and after (**t8**) the bleaching event, indicating that the earlier MC10 inoculation (at **t0**) was associated with the establishment of a microbiome state potentially more favorable for stress response.

Algal symbiont switching (e.g., from sensitive *Cladocopium* to resilient *Durusdinium*) represents a known thermal adaptation pathway in some corals (*47*), but this mechanism is unlikely to explain our results. Region-wide characterization confirms that Hong Kong corals, including *Acropora* spp., predominantly harbor *Cladocopium* spp. (except *O. crispata*) (*48*). This consistent symbiont profile across host species and sites makes algal-mediated thermal tolerance an improbable alternative explanation for the enhanced resilience observed.

Towards scalable probiotic interventions

Coral restoration commonly involves growing fragments in nurseries before outplanting (*49*, *50*). This operational framework is highly compatible with integrating probiotic intervention as a nursery-applied treatment. Our study establishes a pipeline where evolutionary genomics first selects candidates with a high *a priori* potential for long-term host residency. We employed CBASS as a rapid, reproducible assay to obtain an initial functional readout of acute thermal

tolerance. This step helps triage candidates before resource-intensive field trials.

Our 8-month field trial provides a proof-of-concept that evolutionarily selected probiotics can achieve sustained retention and be associated with enhanced stress tolerance during a natural bleaching event. Critical knowledge gaps remain for evaluating long-term restoration success, an issue plaguing coral restoration initiatives globally (*50*). Multi-year data on coral survival, reproductive fitness, and reef-scale outcomes such as biodiversity recovery and structural complexity are essential next steps.

The scalable application of any probiotic requires a favorable ecological risk profile. *Ruegeria* MC10 occurs naturally across multiple coral species, seawater, and sediment, indicating ecological flexibility without rampant proliferation. Several convergent factors suggest a low-risk, self-limiting phenotype aligned with its selected genomic trajectory: consistently low natural abundance, a pseudogenized metabolism that constrains competitive growth outside host tissues, and minimal field-established abundance within coral gastrodermis. The microbiome restructuring observed during bleaching was a transient, fine-scale modulation rather than a dysbiotic takeover. This combination of traits defines a probiotic candidate that integrates into the holobiont without disruptive dominance, a key consideration for safe, multi-species restoration.

The beneficial effects of MC10-B4 in both a model cnidarian and a reef-building coral suggest potential for cross-species efficacy. Further validation across a wider range of coral species, coupled with rigorous evaluation of potential off-target effects, is a necessary next step. Developing high-efficiency, scalable delivery technologies for underwater nursery applications could improve treatment effectiveness. If this approach proves generalizable and safe, such broad-host applicability would significantly enhance scalability. This would enable the same

probiotic preparation to be used across multiple coral species within nursery-based workflows. This initial proof-of-concept points toward a promising avenue for developing scalable, microbial-based interventions to help bridge the resilience gap for coral reefs.

Acknowledgements: We thank all the colleagues who have supported experiments to test physiological priming effect, outplant fieldwork, and FISH experiments, including Jingqi Gao, Kai Yan Lai, and Nikolai B. Tang. We would like to thank Kristin Bär-Häge and Myriam Schmid for their support with Aiptasia animal husbandry for CBASS acute thermal assays.

Funding: Hong Kong Research Grants Council (RGC) General Research Fund project #: 14114724 granted to H.L. Grand Challenges Scheme project #: 4720293 by the CUHK-Exeter Joint Centre for Environmental Sustainability and Resilience (ENSURE) granted to H.L. “Reviving Our Corals” initiative agreement #: TW2318074 by WWF Hong Kong and Coral Academy, The Chinese University of Hong Kong granted to A.P.Y.C. German Research Foundation (DFG) project #: 458901010 granted to C.R.V.

Author Contributions: Conceptualization: H.L. Methodology on *Ruegeria* isolation, genome analysis, and population-level primer design: M.X., T.L., H.L. Methodology on CBASS: C.R.V., N.X. Code development: T.L., X.W. Investigation on coral sampling and *Ruegeria* isolation: M.X., K.E.H., D.L., S.E.M., R.H., E.C., Z.W., P.T., J.B. Investigation on bacterial growth rate: C.J.X., Q.H. Investigation on CBASS: N.X., M.D., H.M., C.R.V. Methodology and investigation on probiotic priming and postbiotic effect: P.L., N.X., C.T.C., M.X., H.L., R.S.P., C.R.V., A.P.Y.C. Field trial: A.P.Y.C., C.T.C., C.H.L, W.Y.T, K.K.T. Methodology on FISH: Z.X., G.C.

Data visualization and statistical analysis: N.X., S.E.M. Funding acquisition: H.L., A.P.Y.C., C.R.V. Project administration: H.L. Supervision: H.L., C.R.V., A.P.Y.C. Writing – original draft: H.L. Writing – review and editing: C.R.V., H.L., N.X., M.X., S.E.M., R.S.P., G.C. Writing – supplementary materials: M.X., N.X., T.L., C.T.C., A.P.Y.C., H.L.

Competing interests: The authors declare that they have no competing interests.

Data and materials availability: The scripts used for genome assembly and annotations, population genomic analysis, amplicon data analysis, and pseudogene analysis have been deposited in an online repository (https://github.com/444thLiao/CoralProbiotic).

References

1. F. J. Gatesoupe, The use of probiotics in aquaculture. *Aquaculture* **180**, 147–165 (1999).

2. L. P. Henry, J. Bergelson, Applying ecological principles to microbiome engineering. *Nature Microbiology* **10**, 2111–2121 (2025).

3. M. Moradi, P. R. Magalhaes, R. S. Peixoto, C. C. Jonck, D. François, A. C. F. Bellot, J. B. Teixeira, C. S. Silveira, G. Duarte, H. Evangelista, Probiotics mitigate thermal stress-and pathogen-driven impacts on coral skeleton. *Frontiers in Marine Science* **10**, 1212690 (2023).

4. B. Ushijima, S. P. Gunasekera, J. L. Meyer, J. Tittl, K. A. Pitts, S. Thompson, J. M. Sneed, Y. Ding, M. Chen, L. Jay Houk, Chemical and genomic characterization of a potential probiotic treatment for stony coral tissue loss disease. *Communications Biology* **6**, 248 (2023).

5. D. A. Goldman, K. S. Xue, A. B. Parrott, J. A. Lopez, J. C. Vila, R. R. Jeeda, L. R. Franzese, R. L. Porter, I. J. Gray, B. C. DeFelice, Competition for shared resources increases dependence on initial population size during coalescence of gut microbial communities. *Proceedings of the National Academy of Sciences* **122**, e2322440122 (2025).

6. W. R. Whitaker, Z. N. Russ, E. Stanley Shepherd, L. M. Popov, A. Louie, K. Lam, D. M. Zong, C. C. Gill, J. L. Gehrig, H. S. Rishi, Controlled colonization of the human gut with a genetically engineered microbial therapeutic. *Science* **389**, 303–308 (2025).

7. D. Russ, C. R. Fitzpatrick, P. J. Teixeira, J. L. Dangl, Deep discovery informs difficult deployment in plant microbiome science. *Cell* **186**, 4496–4513 (2023).

8. S. Čaušević, M. Dubey, M. Morales, G. Salazar, V. Sentchilo, N. Carraro, H.-J. Ruscheweyh, S. Sunagawa, J. R. van der Meer, Niche availability and competitive loss by facilitation control proliferation of bacterial strains intended for soil microbiome interventions. *Nature communications* **15**, 2557 (2024).

9. N. A. Moran, G. R. Plague, Genomic changes following host restriction in bacteria. *Current opinion in genetics & development* **14**, 627–633 (2004).

10. J. Perreau, N. A. Moran, Genetic innovations in animal–microbe symbioses. *Nature Reviews Genetics* **23**, 23–39 (2022).

11. R. Fisher, R. A. O'Leary, S. Low-Choy, K. Mengersen, N. Knowlton, R. E. Brainard, M. J. Caley, Species richness on coral reefs and the pursuit of convergent global estimates. *Current Biology* **25**, 500–505 (2015).

12. D. Souter, S. Planes, J. Wicquart, M. Logan, D. Obura, F. Staub. (Global coral reef monitoring network (GCRMN) and international coral reef …, 2021).

13. J. N. Kittinger, E. M. Finkbeiner, E. W. Glazier, L. B. Crowder, Human dimensions of coral reef social-ecological systems. *Ecology and Society* **17**, (2012).

14. T. P. Hughes, J. T. Kerry, A. H. Baird, S. R. Connolly, A. Dietzel, C. M. Eakin, S. F. Heron, A. S. Hoey, M. O. Hoogenboom, G. Liu, Global warming transforms coral reef assemblages. *Nature* **556**, 492–496 (2018).

15. I. C. Change, Synthesis Report. Contribution of working groups I. *II and III to the fifth assessment report of the intergovernmental panel on climate change* **151**, (2014).

16. N. Rädecker, C. Pogoreutz, H. M. Gegner, A. Cárdenas, F. Roth, J. Bougoure, P. Guagliardo, C. Wild, M. Pernice, J.-B. Raina, Heat stress destabilizes symbiotic nutrient cycling in corals. *Proceedings of the national academy of sciences* **118**, e2022653118 (2021).

17. C. M. Eakin, D. Devotta, S. F. Heron, S. Connolly, G. Liu, E. Geiger, J. D. L. Cour, A. Gomez, W. Skirving, A. H. Baird, The 2014-17 global coral bleaching event: the most severe and widespread coral reef destruction. *Preprint*, (2022).

18. J. D. Reimer, R. S. Peixoto, S. W. Davies, N. Traylor-Knowles, M. L. Short, R. A. Cabral-Tena, J. A. Burt, I. Pessoa, A. T. Banaszak, R. S. Winters, The fourth global coral bleaching event: where do we go from here? *Coral Reefs* **43**, 1121–1125 (2024).

19. M. J. Huggett, A. Apprill, Coral microbiome database: Integration of sequences reveals high diversity and relatedness of coral‐associated microbes. *Environmental microbiology reports* **11**, 372–385 (2019).

20. C. R. Voolstra, J.-B. Raina, M. Dörr, A. Cárdenas, C. Pogoreutz, C. B. Silveira, A. R. Mohamed, D. G. Bourne, H. Luo, S. A. Amin, The coral microbiome in sickness, in health and in a changing world. *Nature Reviews Microbiology* **22**, 460–475 (2024).

21. P. Arevalo, D. VanInsberghe, J. Elsherbini, J. Gore, M. F. Polz, A reverse ecology approach based on a biological definition of microbial populations. *Cell* **178**, 820–834. e814 (2019).

22. M. A. Moran, A. Buchan, J. M. González, J. F. Heidelberg, W. B. Whitman, R. P. Kiene, J. R. Henriksen, G. M. King, R. Belas, C. Fuqua, Genome sequence of Silicibacter pomeroyi reveals adaptations to the marine environment. *Nature* **432**, 910–913 (2004).

23. N. R. Evensen, K. E. Parker, T. A. Oliver, S. R. Palumbi, C. A. Logan, J. S. Ryan, C. N. Klepac, G. Perna, M. E. Warner, C. R. Voolstra, The Coral Bleaching Automated Stress System (CBASS): A low‐cost, portable system for standardized empirical assessments of coral thermal limits. *Limnology and Oceanography: Methods* **21**, 421–434 (2023).

24. M. Dörr, J. Denger, C. S. Maier, J. V. Kirsch, H. Manns, C. R. Voolstra, Short-term heat stress assays resolve effects of host strain, repeat stress, and bacterial inoculation on Aiptasia thermal tolerance phenotypes. *Coral Reefs* **42**, 1271–1281 (2023).

25. S. Baumgarten, O. Simakov, L. Y. Esherick, Y. J. Liew, E. M. Lehnert, C. T. Michell, Y. Li, E. A. Hambleton, A. Guse, M. E. Oates, The genome of Aiptasia, a sea anemone model for coral symbiosis. *Proceedings of the National Academy of Sciences* **112**, 11893–11898 (2015).

26. C. R. Voolstra, R. Alderdice, L. Colin, S. Staab, A. Apprill, J.-B. Raina, Standardized methods to assess the impacts of thermal stress on coral reef marine life. *Annual Review of Marine Science* **17**, (2025).

27. B. J. Callahan, J. Wong, C. Heiner, S. Oh, C. M. Theriot, A. S. Gulati, S. K. McGill, M. K. Dougherty, High-throughput amplicon sequencing of the full-length 16S rRNA gene with single-nucleotide resolution. *Nucleic acids research* **47**, e103–e103 (2019).

28. N. Garcias-Bonet, A. Roik, B. Tierney, F. C. García, H. D. Villela, A. M. Dungan, K. M. Quigley, M. Sweet, G. Berg, L. Gram, Horizon scanning the application of probiotics for wildlife. *Trends in Microbiology* **32**, 252–269 (2024).

29. R. S. Peixoto, M. Sweet, H. D. Villela, P. Cardoso, T. Thomas, C. R. Voolstra, L. Høj, D. G. Bourne, Coral probiotics: premise, promise, prospects. *Annual review of animal biosciences* **9**, 265–288 (2021).

30. T. Doering, J. Maire, M. J. van Oppen, L. L. Blackall, Advancing coral microbiome manipulation to build long-term climate resilience. *Microbiology Australia* **44**, 36–40 (2023).

31. A. S. Fernandes, K. F. Campos, J. C. S. de Assis, O. S. Gonçalves, M. V. d. Queiroz, D. M. S. Bazzolli, M. F. Santana, Investigating the impact of insertion sequences and transposons in the genomes of the most significant phytopathogenic bacteria. *Microbial Genomics* **10**, 001219 (2024).

32. P. Siguier, E. Gourbeyre, M. Chandler, Bacterial insertion sequences: their genomic impact and diversity. *FEMS microbiology reviews* **38**, 865–891 (2014).

33. M. Xie, N. Xiang, T. Liao, C. T. Cheung, C. H. Lee, W. Y. Tse, K. K. Tsang, K. E. Ho, Q. He, M. Dörr, Evolutionary Genomics Guides Scalable Coral Probiotics for Climate Resilience. *bioRxiv*, 2025.2006. 2016.659728 (2025).

34. J. H. Lee, F. Arega, Eutrophication dynamics of Tolo Harbour, Hong Kong. *Marine Pollution Bulletin* **39**, 187–192 (1999).

35. L. Broudic, M. Pinault, R. Claud, T. Bajjouk, T. Rungassamy, N. Nikolic, E. Crochelet, C. Mazé, B. Bergerot, Mapping benthic biodiversity indicators of coral reefs using spatial interpolation. *Coral Reefs*, 1–18 (2025).

36. T. Cyronak, Y. Takeshita, T. A. Courtney, E. H. DeCarlo, B. D. Eyre, D. I. Kline, T. Martz, H. Page, N. N. Price, J. Smith, Diel temperature and pH variability scale with depth across diverse coral reef habitats. *Limnology and Oceanography Letters* **5**, 193–203 (2020).

37. M. R. de Souza, C. Caruso, L. Ruiz-Jones, C. Drury, R. D. Gates, R. J. Toonen, Importance of depth and temperature variability as drivers of coral symbiont composition despite a mass bleaching event. *Scientific Reports* **13**, 8957 (2023).

38. G. Lajoie, L. W. Parfrey, Beyond specialization: re-examining routes of host influence on symbiont evolution. *Trends in Ecology & Evolution* **37**, 590–598 (2022).

39. K. Gutiérrez-García, K. Aumiller, R. Dodge, B. Obadia, A. Deng, S. Agrawal, X. Yuan, R. Wolff, H. Zhu, R.-C. Hsia, A conserved bacterial genetic basis for commensal-host specificity. *Science* **386**, 1117–1122 (2024).

40. D.-W. Kang, J. B. Adams, D. M. Coleman, E. L. Pollard, J. Maldonado, S. McDonough-Means, J. G. Caporaso, R. Krajmalnik-Brown, Long-term benefit of Microbiota Transfer Therapy on autism symptoms and gut microbiota. *Scientific reports* **9**, 5821 (2019).

41. L. S. McKee, S. L. La Rosa, B. Westereng, V. G. Eijsink, P. B. Pope, J. Larsbrink, Polysaccharide degradation by the Bacteroidetes: mechanisms and nomenclature. *Environmental Microbiology Reports* **13**, 559–581 (2021).

42. A. Pavlopoulou, G. D. Savva, M. Louka, P. G. Bagos, C. E. Vorgias, I. Michalopoulos, A. G. Georgakilas, Unraveling the mechanisms of extreme radioresistance in prokaryotes: lessons from nature. *Mutation Research/Reviews in Mutation Research* **767**, 92–107 (2016).

43. Y.-W. Lien, D. Amendola, K. S. Lee, N. Bartlau, J. Xu, G. Furusawa, M. F. Polz, R. Stocker, G. L. Weiss, M. Pilhofer, Mechanism of bacterial predation via ixotrophy. *Science* **386**, eadp0614 (2024).

44. M. Ksiezarek, F. Grosso, T. G. Ribeiro, L. Peixe, Genomic diversity of genus Limosilactobacillus. *Microbial Genomics* **8**, 000847 (2022).

45. S. M. Zhang, J. H. Hung, T. N. Yen, S. L. Huang, Mutualistic interactions of lactate‐producing lactobacilli and lactate‐utilizing Veillonella dispar: Lactate and glutamate cross‐feeding for the enhanced growth and short‐chain fatty acid production. *Microbial Biotechnology* **17**, e14484 (2024).

46. J. L. Matthews, J. B. Raina, T. Kahlke, J. R. Seymour, M. J. van Oppen, D. J. Suggett, Symbiodiniaceae‐bacteria interactions: rethinking metabolite exchange in reef‐building corals as multi‐partner metabolic networks. *Environmental Microbiology* **22**, 1675−1687 (2020).

47. K. M. Quigley, B. Ramsby, P. Laffy, J. Harris, V. J. Mocellin, L. K. Bay, Symbioses are restructured by repeated mass coral bleaching. *Science Advances* **8**, eabq8349 (2022).

48. O. S. Saad, X. Lin, T. Y. Ng, L. Li, P. Ang, S. Lin, Species richness and generalists–specialists mosaicism of symbiodiniacean symbionts in corals from Hong Kong revealed by high-throughput ITS sequencing. *Coral Reefs* **41**, 1–12 (2022).

49. D. J. Suggett, M. J. van Oppen, Horizon scan of rapidly advancing coral restoration approaches for 21st century reef management. *Emerging Topics in Life Sciences* **6**, 125–136 (2022).

50. L. Boström-Einarsson, R. C. Babcock, E. Bayraktarov, D. Ceccarelli, N. Cook, S. C. Ferse, B. Hancock, P. Harrison, M. Hein, E. Shaver, Coral restoration–A systematic review of current methods, successes, failures and future directions. *PloS one* **15**, e0226631 (2020).

619

Figure legends

Fig. 1 *Ruegeria* MC10's phylogenetic position and genomic signatures showing recent host dependency, along with free-living physiological cost. (A) Rooted maximum-likelihood phylogenomic tree comprising 419 *Ruegeria* isolates associated with five coral species sampled from nine Hong Kong reef sites, along with 26 *Ruegeria* genomes retrieved from public databases. This tree was constructed with IQ-TREE based on concatenated single-copy orthologous genes at the amino acid level. PopCOGenT was used to delineate the *Ruegeria* populations (i.e., main clusters or MCs). The 19 MCs that contain representative members additionally sequenced by Nanopore were labelled with numbers in the tree. From the inner to outer rings: (1) denotes 29 *Ruegeria* populations which consists of at least three isolates as defined by PopCOGenT, along with MC46, the sister group of MC10; (2) - (5) denote the source of *Ruegeria* isolates with each corresponding to coral species, sampling site, coral compartment, and coral colony replicate, respectively. **(B)** Stacked bars showing the number of IS and IS family composition in 34 newly closed *Ruegeria* genomes and the reference genome *Ruegeria pomeroyi* DSS-3. **(C)** Number of pseudogenes in 34 newly closed *Ruegeria* genomes and the reference genome *R. pomeroyi* DSS-3. Pseudogenes were grouped by the mechanism of formation, namely "IS disruption", "Frameshift mutations", "Nonsense mutations", and "Singletons". "Unclassified" pseudogenes are those that cannot be assigned to any of the three defined mechanisms. (D) Maximum growth rate (μ_{max}, h^{-1}) comparison. Bars represent the mean μ_{max} ± standard deviation of the MC10 population, the non-MC10 *Ruegeria* population and a free-living model *R. pomeroyi* DSS-3. Growth rates were calculated from the exponential phase of growth curves. Significant difference (PhylANOVA with Brownian motion evolution model, $P = 0.009$) was observed in growth rates between MC10 versus non-MC10 counterparts.

Fig. 2 Relative abundance of *Ruegeria* MC10 in coral holobionts and environmental samples from Hong Kong reefs. (A) The relative abundance of MC10 in *Ruegeria* communities was quantified based on population-resolving *ATP5B* and *parC* amplicon sequencing across natural reefs in Hong Kong. Different bar plots under the same coral genus represented for different coral colonies (i.e., 15 colonies for *Oulastrea* sp., 11 for *Platygyra* sp., 10 colonies for *Porites* sp., 4 colonies for *Acropora* sp., and 4 colonies for *Plesiastrea* sp. across five sites). Each bar plot was displayed with the mean value and standard deviation (SD) calculated from three compartments (i.e., mucus, tissue and skeleton) for the same coral colony. **(B)** The relative abundance of MC10 in seawater and sediment samples across different locations. The error bar denotes standard deviation among three replicates. CI, Crescent Island; SI, Sharp Island; WP, Wu Pai. Sd, sediment; Sw, seawater.

Fig. 3 Application of *Ruegeria* MC10-B4 through laboratory and field trials. (A, B) Results of laboratory CBASS assay on *Exaiptasia diaphana*; **(A)** ED50 values of Aiptasia H2 inoculated with *Ruegeria* MC10-B4 or placebo FSW after heat stress (T7) and post-stress recovery (T18). Data were presented with the mean values and standard errors. **(B)** ED50 values modeled based on log-logistic regression curves of dark-adapted photosynthetic efficiency (F_v/F_m) across experimental temperatures. F_v/F_m was measured at 7 h and 18 h of the CBASS with one-hour dark acclimation. Treatment-specific ED50 values were denoted as vertical lines. (**C-G**) Results of field trials on coral Acropora pruinosa. The relative abundance of **(C)** MC10 and **(D)** MC15 in the *Ruegeria* (left axis; based on *parC* amplicon) and total bacteria community (right axis; combined 16S rRNA and *parC* gene amplicon) following twice-weekly inoculations over a month. The central line of each box indicates the median value with the upper and lower error bar showing maximum and minimum potential variabilities, respectively. **(E)** Coral phenotype

and coloration, and **(F)** effective quantum yield (F_v'/F_m') were assessed on MC10-B4-inoculated and placebo-treated corals across five timepoints: 1, 3, 6, 7 and 8 months post-outplanting (t1, t3, t6, t7, t8, respectively). Data were presented with the mean values and standard errors. **(G)** Localization of MC10 in coral *A. pruinosa* after one-month inoculations (t0, before outplanting), six months post-outplanting (t6, during bleaching), and eight months post-outplanting (t8, post-bleaching). Representative confocal images depicting the hybridization of high-resolution *parC* probe specifically targeting MC10 labeled with Cy3 (purple). The purple arrows pointed at the specific location of MC10 in the coral gastrodermis. The blue arrows pointed at the non-specific binding sites. The yellow arrows pointed at Symbiodiniaceae. Grey, DAPI-stained dsDNA; Green, autofluorescence of Symbiodiniaceae; Scale bars, 10 μm. Gd, gastrodermis; ep, epidermis; sym, Symbiodiniaceae. All significant differences were indicated in bold and marked with asterisks (***: $P < 0.001$, **: $P < 0.01$; *: $P < 0.05$; n.s.: non-significant).

Fig. 4 Coral microbiome dynamics during field trial. (A) Principal Coordinates Analysis (PCoA) of coral holobiont-associated bacterial communities based on Bray-Curtis dissimilarity, comparing placebo and MC10-B4-treated groups across five timepoints: baseline (t0, pre-outplanting) and 1, 3, 6, and 8 months post-outplanting (t1, t3, t6, t8, respectively). Ellipses represent 95% confidence intervals for group centroids. ANOSIM was used to assess the separation of the placebo and MC10-B4-treated groups, with R values interpreted as: little to no ($R < 0.25$), weak ($0.25 \leq R < 0.5$), moderate ($0.5 \leq R < 0.75$), and strong ($R \geq 0.75$). **(B)** Differentially abundant taxa between placebo and MC10-B4-treated corals at t6 (during bleaching) identified by ANCOM-BC analysis ($P < 0.05$, FDR corrected). A heatmap displaying top 20 significantly upregulated (positive log2FC) and downregulated (negative log2FC) genera, respectively. A log2-transformed read counts (log2[reads+1]) were shown to indicate the

absolute fold-change magnitudes of taxa. Pseudocounts were added to handle the case of zeros in the calculation.

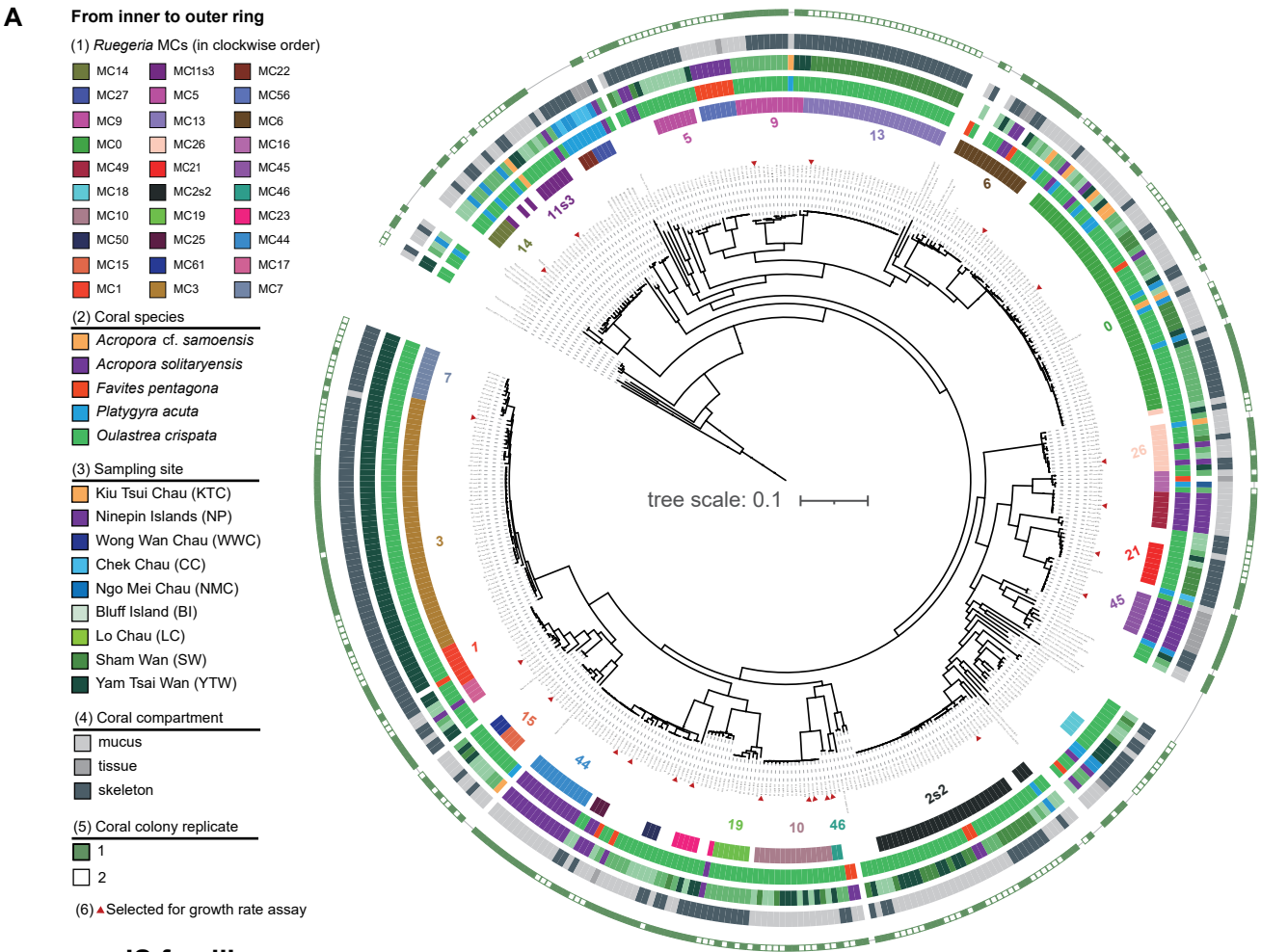
A
From inner to outer ring
(1) Ruegeria MCs (in clockwise order)
MC14
MC11s3
MC22
MC27
MC5
MC56
MC9
MC13
MC6
MC0
MC26
MC16
MC49
MC21
MC45
MC18
MC2s2
MC46
MC10
MC19
MC23
MC50
MC25
MC44
MC15
MC61
MC17
MC1
MC3
MC7
(2) Coral species
Acropora cf. samoensis
Acropora solitaryensis
Favites pentagona
Platygyra acuta
Oulastrea crispata
(3) Sampling site
Kiu Tsui Chau (KTC)
Ninepin Islands (NP)
Wong Wan Chau (WWC)
Chek Chau (CC)
Ngo Mei Chau (NMC)
Bluff Island (BI)
Lo Chau (LC)
Sham Wan (SW)
Yam Tsai Wan (YTW)
(4) Coral compartment
mucus
tissue
skeleton
(5) Coral colony replicate
1
2
(6) Selected for growth rate assay
tree scale: 0.1

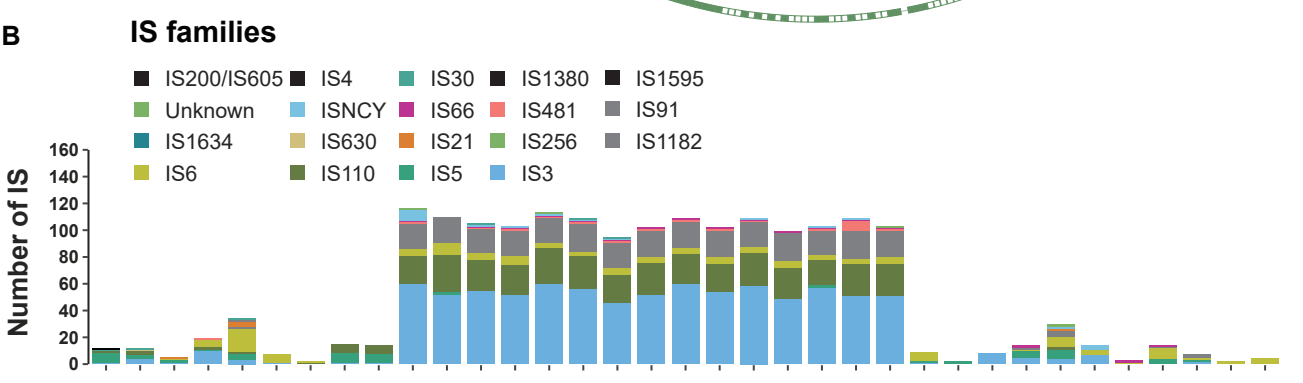
B
IS families
IS200/IS605
IS4
IS30
IS1380
IS1595
Unknown
ISNCY
IS66
IS481
IS91
IS1634
IS630
IS21
IS256
IS1182
IS6
IS110
IS5
IS3
Number of IS
160
140
120
100
80
60
40
20
0

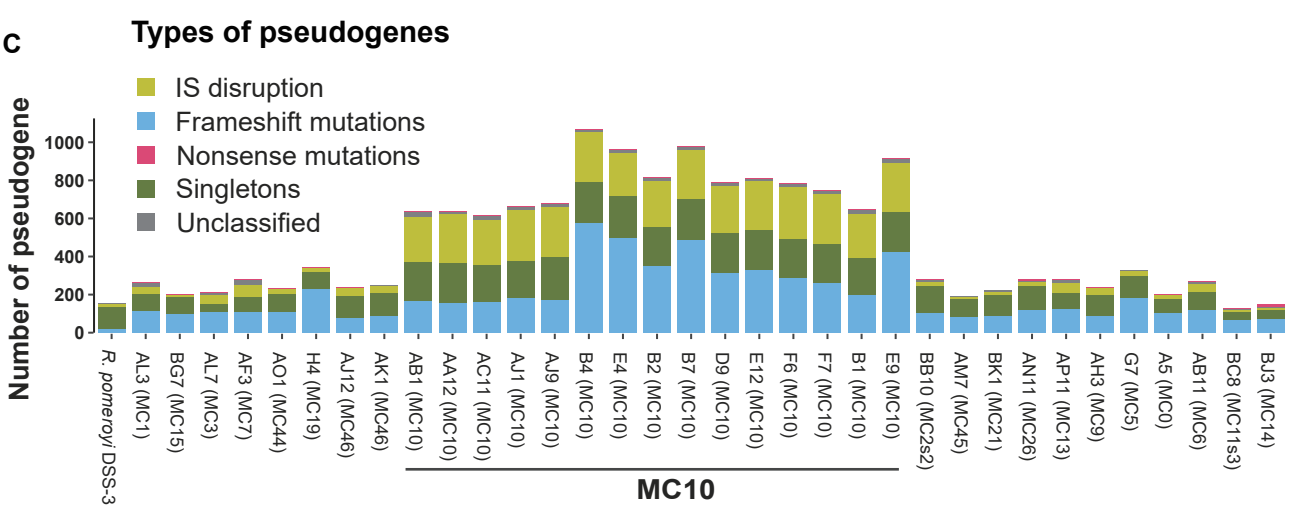
C
Types of pseudogenes
IS disruption
Frameshift mutations
Nonsense mutations
Singletons
Unclassified
Number of pseudogene
1000
800
600
400
200
0
R. pomeroyi DSS-3
AL3 (MC1)
BG7 (MC15)
AL7 (MC3)
AF3 (MC7)
AO1 (MC44)
H4 (MC19)
AJ12 (MC46)
AK1 (MC46)
AB1 (MC10)
AA12 (MC10)
AC11 (MC10)
AJ1 (MC10)
AJ9 (MC10)
B4 (MC10)
E4 (MC10)
B2 (MC10)
B7 (MC10)
D9 (MC10)
E12 (MC10)
F6 (MC10)
F7 (MC10)
B1 (MC10)
E9 (MC10)
BB10 (MC2s2)
AM7 (MC45)
BK1 (MC21)
AN11 (MC26)
AP11 (MC13)
AH3 (MC9)
G7 (MC5)
A5 (MC0)
AB11 (MC6)
BC8 (MC11s3)
BJ3 (MC14)
MC10

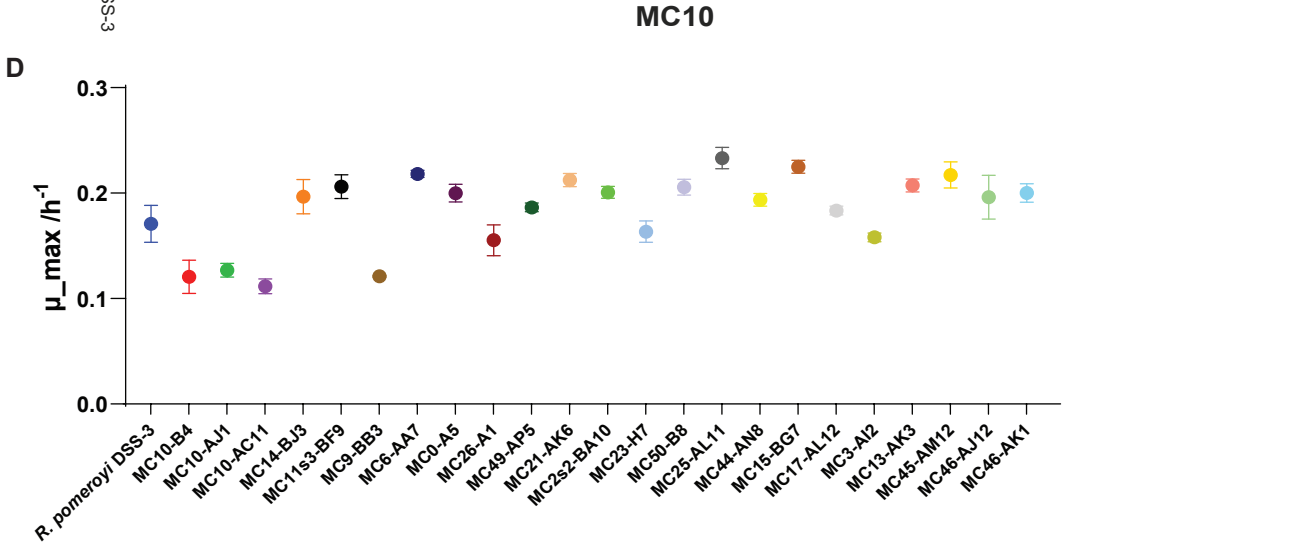
D
μ_max /h-1
0.3
0.2
0.1
0.0
R. pomeroyi DSS-3
MC10-B4
MC10-AJ1
MC10-AC11
MC14-BJ3
MC11s3-BF9
MC9-BB3
MC6-AA7
MC0-A5
MC26-A1
MC49-AP5
MC21-AK6
MC2s2-BA10
MC23-H7
MC50-B8
MC25-AL11
MC44-AN8
MC15-BG7
MC17-AL12
MC3-AI2
MC13-AK3
MC45-AM12
MC46-AJ12
MC46-AK1

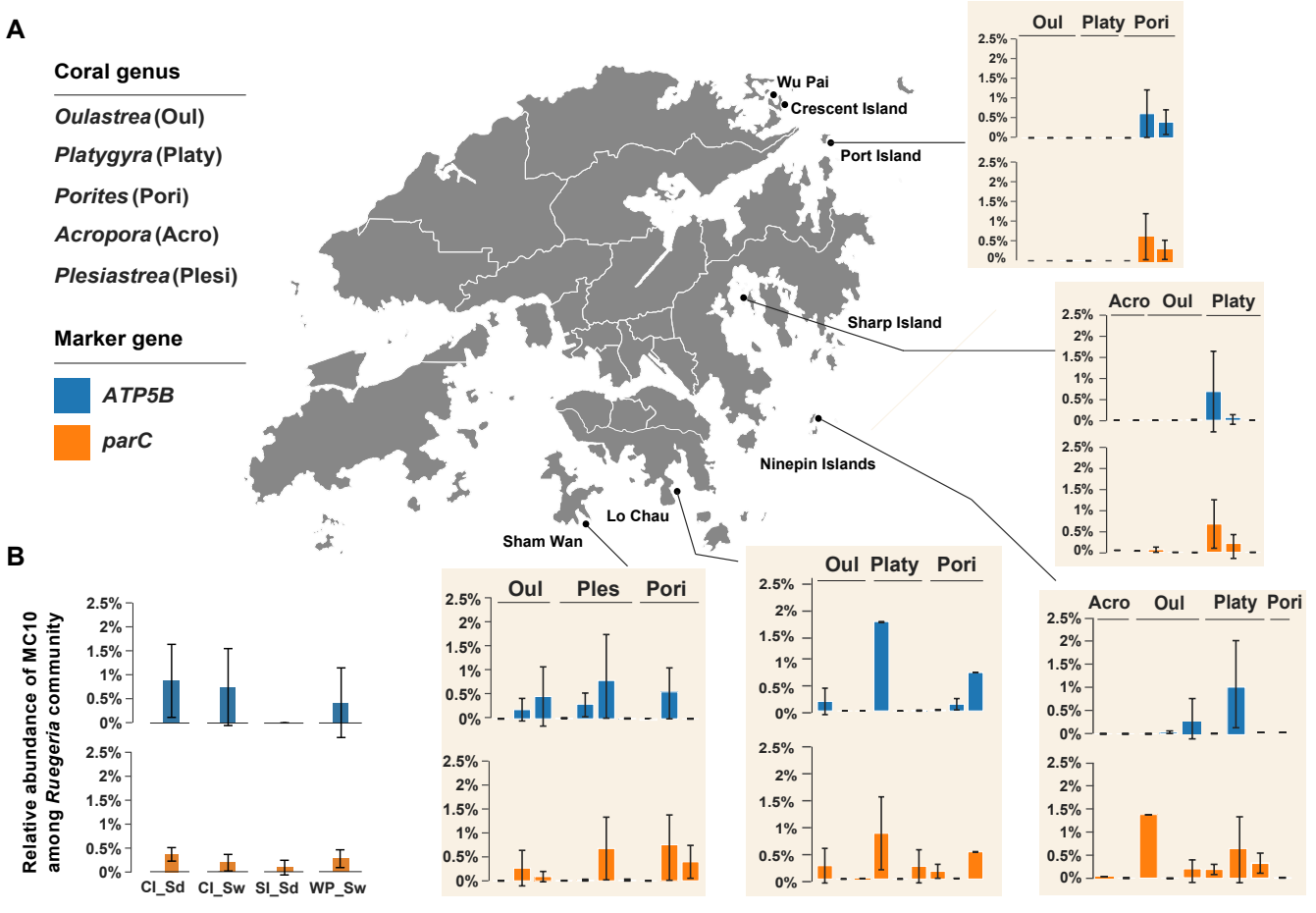
A
Coral genus
Oulastrea (Oul)
Platygyra (Platy)
Porites (Pori)
Acropora (Acro)
Plesiastrea (Plesi)
Marker gene
ATP5B
parC
Wu Pai
Crescent Island
Port Island
Sharp Island
Ninepin Islands
Lo Chau
Sham Wan
Oul Platy Pori
Acro Oul Platy
Oul Ples Pori
Oul Platy Pori
Acro Oul Platy Pori
2.5%
2%
1.5%
1%
0.5%
0%
B
Relative abundance of MC10 among Ruegeria community
Cl_Sd
Cl_Sw
Sl_Sd
WP_Sw

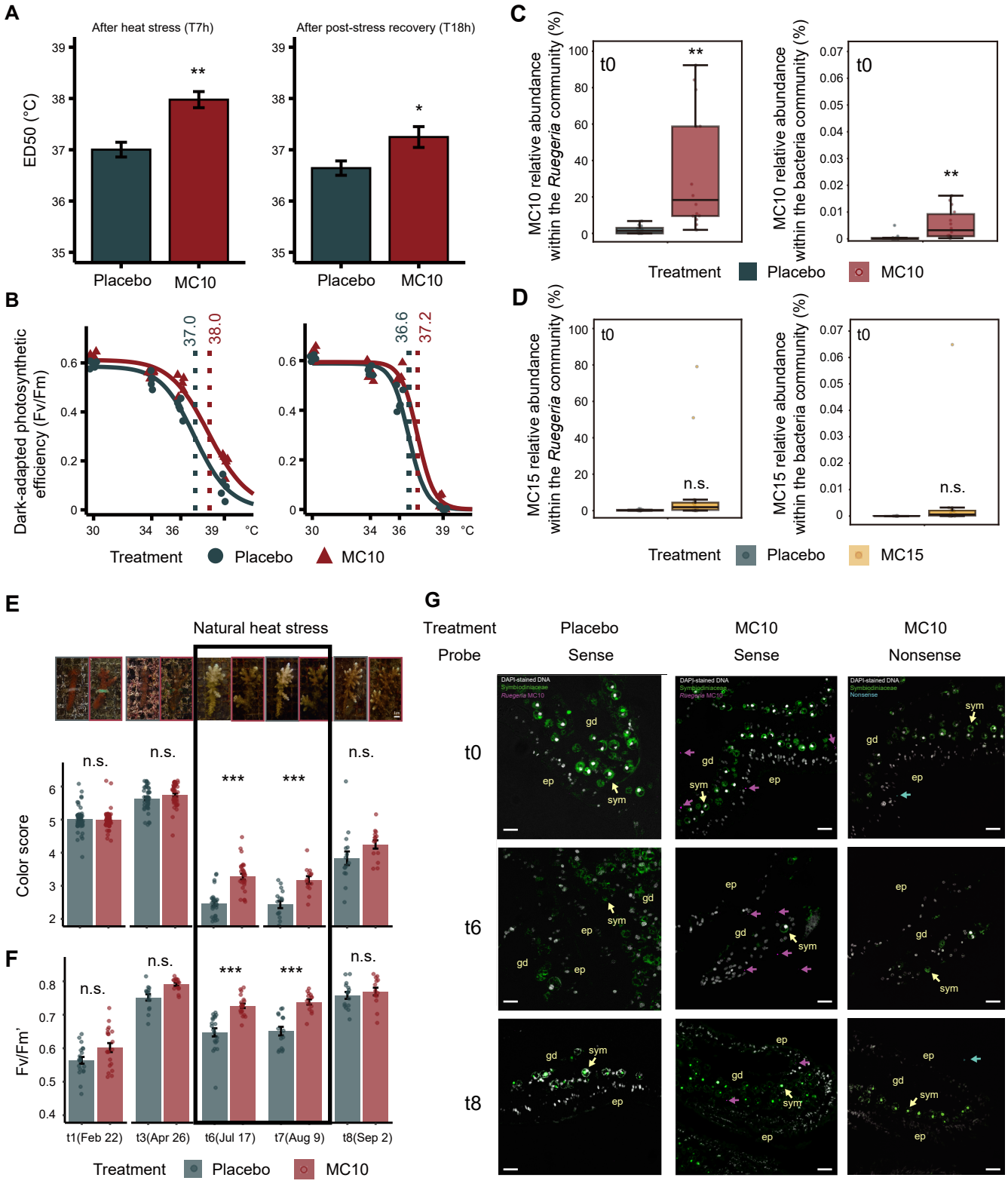
A
After heat stress (T7h)
After post-stress recovery (T18h)
ED50 (°C)
Placebo
MC10
B
Dark-adapted photosynthetic efficiency (Fv/Fm)
37.0
38.0
36.6
37.2
°C
Treatment
Placebo
MC10
C
MC10 relative abundance within the Ruegeria community (%)
MC10 relative abundance within the bacteria community (%)
t0
Treatment
Placebo
MC10
D
MC15 relative abundance within the Ruegeria community (%)
MC15 relative abundance within the bacteria community (%)
n.s.
MC15
E
Natural heat stress
Color score
F
Fv/Fm'
t1(Feb 22)
t3(Apr 26)
t6(Jul 17)
t7(Aug 9)
t8(Sep 2)
G
Treatment
Probe
Placebo
Sense
MC10
Sense
MC10
Nonsense
t0
t6
t8
gd
ep
sym

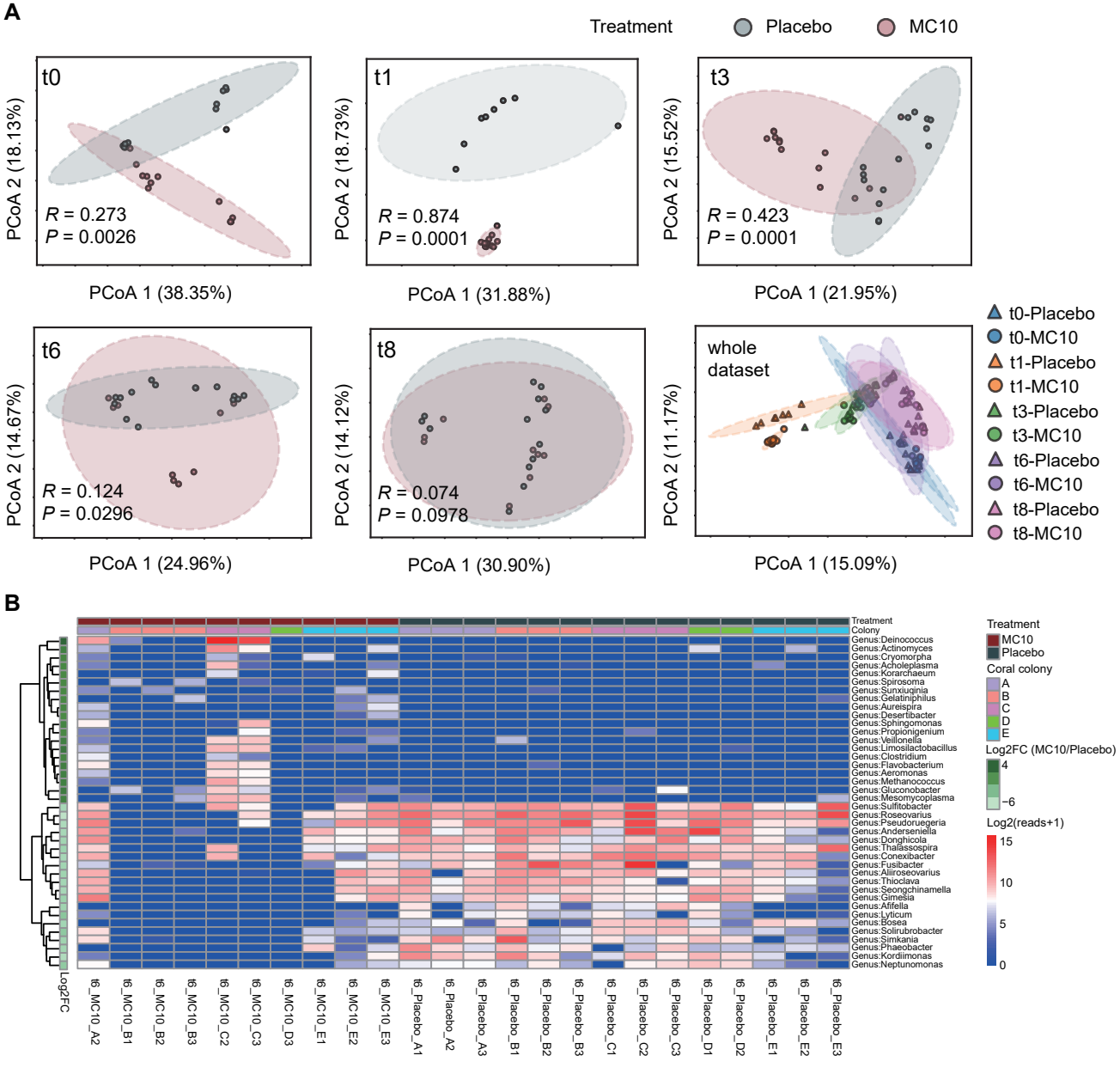
A
Treatment
Placebo
MC10
t0
R = 0.273
P = 0.0026
PCoA 2 (18.13%)
PCoA 1 (38.35%)
t1
R = 0.874
P = 0.0001
PCoA 2 (18.73%)
PCoA 1 (31.88%)
t3
R = 0.423
P = 0.0001
PCoA 2 (15.52%)
PCoA 1 (21.95%)
t6
R = 0.124
P = 0.0296
PCoA 2 (14.67%)
PCoA 1 (24.96%)
t8
R = 0.074
P = 0.0978
PCoA 2 (14.12%)
PCoA 1 (30.90%)
whole dataset
PCoA 2 (11.17%)
PCoA 1 (15.09%)
t0-Placebo
t0-MC10
t1-Placebo
t1-MC10
t3-Placebo
t3-MC10
t6-Placebo
t6-MC10
t8-Placebo
t8-MC10
B
Treatment
Colony
Log2FC
Genus:Deinococcus
Genus:Actinomyces
Genus:Cryomorpha
Genus:Acholeplasma
Genus:Korarchaeum
Genus:Spirosoma
Genus:Sunxiuqinia
Genus:Gelatiniphilus
Genus:Aureispira
Genus:Desertibacter
Genus:Sphingomonas
Genus:Propionigenium
Genus:Veillonella
Genus:Limosilactobacillus
Genus:Clostridium
Genus:Flavobacterium
Genus:Aeromonas
Genus:Methanococcus
Genus:Gluconobacter
Genus:Mesomycoplasma
Genus:Sulfitobacter
Genus:Roseovarius
Genus:Pseudoruegeria
Genus:Anderseniella
Genus:Donghicola
Genus:Thalassospira
Genus:Conexibacter
Genus:Fusibacter
Genus:Aliiroseovarius
Genus:Thioclava
Geongchamamella
Genus:Gimesia
Genus:Afifella
Genus:Lyticum
Genus:Bosea
Genus:Solirubrobacter
Genus:Simkania
Genus:Phaeobacter
Genus:Kordiimonas
Genus:Neptunomonas
t6_MC10_A2
t6_MC10_B1
t6_MC10_B2
t6_MC10_B3
t6_MC10_C2
t6_MC10_C3
t6_MC10_D3
t6_MC10_E1
t6_MC10_E2
t6_MC10_E3
t6_Placebo_A1
t6_Placebo_A2
t6_Placebo_A3
t6_Placebo_B1
t6_Placebo_B2
t6_Placebo_B3
t6_Placebo_C1
t6_Placebo_C2
t6_Placebo_C3
t6_Placebo_D1
t6_Placebo_D2
t6_Placebo_E1
t6_Placebo_E2
t6_Placebo_E3
Treatment
MC10
Placebo
Coral colony
A
B
C
D
E
Log2FC (MC10/Placebo)
4
−6
Log2(reads+1)
15
10
5
0